Volume 1 | Number 1 | Jan 2013 | Pages 1–100

ChemComm

Chemical Communications
www.rsc.org/chemcomm

ROYAL SOCIETY OF CHEMISTRY

This is an *Accepted Manuscript*, which has been through the Royal Society of Chemistry peer review process and has been accepted for publication.

Accepted Manuscripts are published online shortly after acceptance, before technical editing, formatting and proof reading. Using this free service, authors can make their results available to the community, in citable form, before we publish the edited article. We will replace this *Accepted Manuscript* with the edited and formatted *Advance Article* as soon as it is available.

You can find more information about *Accepted Manuscripts* in the **Information for Authors**.

Please note that technical editing may introduce minor changes to the text and/or graphics, which may alter content. The journal's standard **Terms & Conditions** and the **Ethical guidelines** still apply. In no event shall the Royal Society of Chemistry be held responsible for any errors or omissions in this *Accepted Manuscript* or any consequences arising from the use of any information it contains.

Journal Name

COMMUNICATION

Ethanol Induces the Formation of Water-Permeable Defects in Model Bilayers of Skin Lipids

R. Thind,[a] D. W. O'Neill,[a] A. Del Regno[a] and R. Notman*[a]

We show that ethanol can induce the formation of water-permeable defects in model membranes of skin, providing a fresh perspective on ethanol as a membrane modulator. We rationalise our findings in terms of the chemical nature of ethanol, *i.e.*, a combination of its hydrogen bonding propensity and amphiphilic character.

Many small molecules are able to interact with biological lipid membranes and modulate their structural and dynamic properties and phase behaviour. This can have important consequences for normal membrane functions such as transport and signalling. Ethanol (EtOH) is a well-known membrane modulator. For example, the anaesthetic effects of EtOH have been attributed in part to its effects on the lateral pressure of cell membranes, which in turn changes the activity of embedded membrane proteins [1]. Furthermore, EtOH is a penetration enhancer (PE) that promotes the transport of molecules through skin. Hence it is used in a number of pharmaceutical creams and patches to facilitate transdermal drug delivery [2]. Despite its effects on skin, everyday exposure to EtOH is widespread. For example EtOH is a major component of antiseptic gels and handwashes; yet it can lower the skin's natural defences and cause irritation. EtOH is also excreted in sweat during normal social drinking, which may be responsible for some of its toxicological effects [3]. While it is known that EtOH partitions into the lipid layers of skin [4], the mechanism by which it enhances penetration remains unclear. An understanding of the mechanism of action of EtOH will assist in the rational design of novel PEs or retarders as well as enabling a proper assessment of the effects of exposure of skin and other biological membranes to EtOH.

The main barrier component of skin (located in the stratum corneum, SC) comprises multiple layers of intercellular lipids (predominantly ceramides, cholesterol and free fatty acids) in a gel phase. PEs are molecules that reversibly interact with these lipid layers to modulate the barrier properties of skin. They may act *via* a number of different mechanisms such as fluidisation, membrane thinning or phase separation [5]. EtOH is known to partition into skin and enhance the permeation of both polar and nonpolar molecules [4-6]. A number of studies point to lipid extraction, and thus membrane damage, as the mechanism of action of EtOH [4, 6], although this mechanism does not sufficiently explain why enhancement is greater for some molecules than others. As EtOH has been found to disorder the hydrocarbon chain regions of phospholipid bilayers, fluidisation of the skin lipids by EtOH has been hypothesised [6]; however FTIR spectroscopy does not detect lipid fluidisation in pure ceramide films [7], synthetic skin-lipid mixtures [8] or in real skin samples [6, 9].

Molecular dynamics (MD) computer simulations offer a powerful route to understanding the mechanisms of action of membrane modulators at the molecular level. Indeed, the effects of EtOH on phospholipid bilayers are well studied by simulations [10]. The skin lipids have so far received less attention; however interest in this area is growing rapidly and has seen the recent development of a number of skin lipid models *e.g.* Refs [11, 12] and application of these models to the study of membrane modulators such as DMSO [12, 13].

In this communication we report MD simulations to determine the effects of EtOH on the properties of ceramide 2 (CER2, ESI Figure 1) bilayers. As CER2 is one of the most abundant lipids in the skin, CER2 bilayers are a useful starting point for modelling the SC lipid layers before moving on to more complex lipid mixtures. We have simulated CER2 bilayers in EtOH-water mixtures, ranging from pure water to pure EtOH. To quantify the effect of EtOH on the water transport properties of the bilayer we have also computed the free energy profile of a water molecule as it crosses the bilayer in both a pure water and 5:5 EtOH:water mixture. Full details of the simulation methodologies and analyses are provided in the Electronic Supplementary Information (ESI).

Snapshots of each bilayer in an EtOH-water mixture at the end of the simulations are presented in Figure 1 (all simulation snapshots were generated using PyMOL [14]). A snapshot of the CER2 bilayer in pure water is given in ESI Figure 5. Its structure has been discussed in
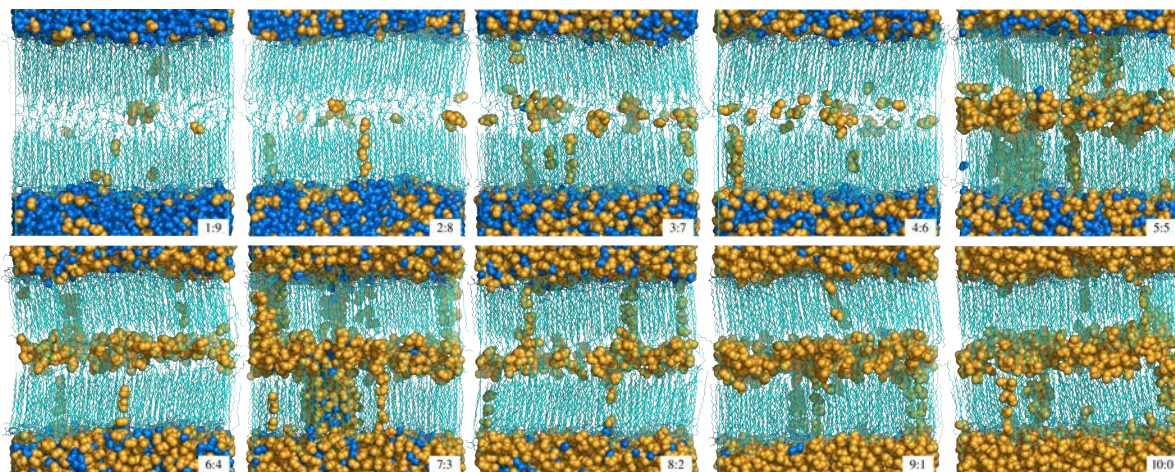
Figure 1 Snapshots of CER2 bilayers in EtOH-water mixtures after at least 100 ns of MD simulation. The ratio of EtOH:water molecules is shown in the bottom right corner of each snapshot. CER2 molecules are coloured in cyan, water molecules in blue and EtOH molecules in orange.

detail in our previous work [12]. In brief, CER2 in water forms a hexagonally-packed gel-phase with highly-ordered tailgroups. A network of H-bonds is present between CER2 headgroups, which helps to maintain the overall integrity of the bilayer. There is an asymmetry in the length of the CER2 hydrocarbon chains that gives rise to a fluid-like region in the centre of the bilayer. For all concentrations of EtOH we observe that EtOH molecules are able to penetrate the bilayer, where they accumulate in the bilayer interior. As EtOH starts to penetrate the bilayer it forms local defects that facilitate the penetration of additional EtOH molecules. This results in the formation of chains of EtOH that span from the solvent phase to the bilayer interior. These defects provide a hydrophilic pathway along which water molecules can travel from one side of the membrane to the other. *Transport along EtOH-induced membrane defects may explain the mechanism by which EtOH enhances the permeation of active molecules through skin.*

To examine further the effect of EtOH on CER2 bilayers we computed a number of bilayer properties. Density profiles of CER2, water and EtOH as a function of the distance along the bilayer normal (z direction) are presented in Figure 2. For all bilayers, the density of water is highest in the solvent phase; there is then a sharp decrease at the bilayer-water interface. In the bilayer in pure water, the water concentration in the bilayer drops to zero beyond the interface. In the bilayers with EtOH there is a small but finite amount of water in the interior of the bilayer, consistent with the presence of water in the EtOH-induced defects. In bilayers with higher concentrations of EtOH ($\geq$5:5 EtOH:water) we occasionally observe the formation of larger EtOH-filled pores (see snapshots of the 5:5 and 7:3 EtOH:water systems in Figure 1). These larger pores enable a slightly greater accumulation of water in the bilayer interior. The density profile of EtOH follows a similar trend to that of water. At low EtOH:water ratios ($\leq$4:6 EtOH:water) there is a small peak in the EtOH density at the interface. This indicates that EtOH has an affinity for the CER2 headgroups, possibly through H-bonding. Indeed, as the concentration of EtOH increases, the number of CER2-EtOH H-bonds increases, while the number of CER2-water H-bonds decreases (ESI Figure 6). Thus, EtOH is essentially dehydrating the membrane. This is in agreement with FTIR spectra of EtOH-treated skin that also indicate reduced H-bonding between water and SC lipids [6]. (We also see a marginal increase in CER2-CER2 H-bonding (ESI Figure 6), which is consistent with Raman spectra of CER2 films in EtOH-water mixtures [15].) The presence of EtOH in the densely-packed region of the CER2 hydrocarbon chains and in the interior of the membrane can also be clearly seen.

The snapshots of the bilayers (Figure 1) and the similarity in the shape of the CER2 density profile for different EtOH concentrations (Figure 2) suggest that the bilayer remains in the ordered gel phase and that EtOH does not act as an archetypal membrane fluidiser. This is consistent with FTIR studies that showed no significant effect of EtOH-water mixtures on the organisation of CER2 hydrocarbon chains [7]. Lipid tail order parameters that reveal the alignment of the CER2 chains with the bilayer normal are presented in ESI Figure 7. For bilayers with low concentrations of EtOH there is some increase in the disorder of the C24 chains close to the headgroups, which may be a consequence of EtOH binding to the CER2 headgroups. For bilayers with high concentrations of EtOH there is an increase in disorder of both chains, however the results are still overall indicative of a gel rather than a fluid phase. At low concentrations, EtOH does not have a significant effect on the thickness of the bilayer and there is only a slight increase (less than 0.05 nm^2 per lipid) in the total cross-sectional area of the bilayer due to the presence of the EtOH-induced defects (ESI Figures 8 and 9). At higher concentrations, the accumulation of water and EtOH in the bilayer interior causes a slight thickening of the bilayer (ESI Figure8). The total cross-sectional area of the bilayer also increases
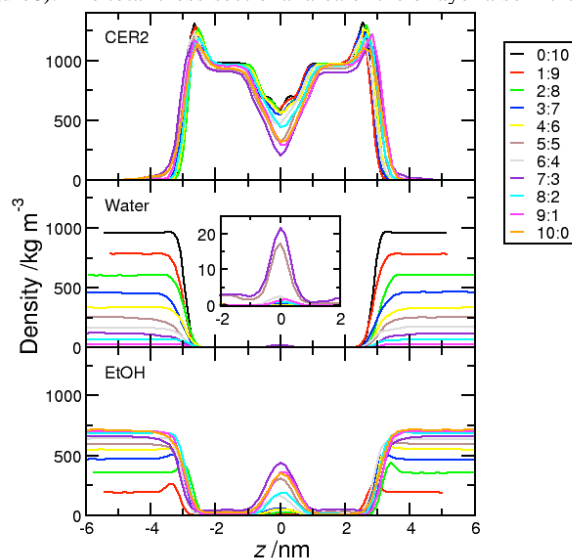

Figure 2 Density profiles of CER2, water and EtOH as a function of the distance along the bilayer normal (z axis of the simulation cell) for bilayers in different EtOH:water mixtures. The inset shows the water density in the bilayer interior.

due to the formation of small defects and larger pores; however elimination of the contribution from defects and pores shows that at high EtOH concentrations the area per lipid actually decreases (ESI Figure 9). Further inspection of the trajectories shows that this is due to either partial or full extraction of CER2 molecules from the bilayer into the solvent phase, *vide infra.*

A snapshot of the bilayer in the 7:3 EtOH:water mixture is shown in Figure 3. This is an example of one of the systems that formed both small defects and a larger pore. It can be seen that two CER2 molecules have been fully extracted from the bilayer into the solvent phase. In addition a number of CER2 molecules have been partially extracted from the bilayer, with one chain remaining embedded in the bilayer and the other chain protruding into the solvent. Overall this results in a decrease in the area per lipid as only one CER2 chain, rather than two, is contributing to the total lipid area. Overlaying Figures 1 and 3 shows that the location of the partially extracted CER2 molecules corresponds to the location of the defects and pores in the bilayer. It appears that because the hydrocarbon chains are soluble in EtOH, when a chain is in the vicinity of a defect it is able to move along the defect and out into the solvent phase. Further examples of lipid extraction in the bilayers in high concentrations of EtOH are given in ESI Figure 10. Lipid extraction by EtOH has been also observed in experiments on real skin samples [4, 6]. Furthermore, experiments on synthetic mixtures of skin lipids showed that while EtOH caused some lipid extraction, the packing of the remaining lipids was not perturbed at physiologically-relevant temperatures [8].

To quantify the effect of EtOH on the water transport properties of the membrane, the free energy profile of a water molecule as a function of its perpendicular distance to the centre of mass of the bilayer was computed for the bilayer in pure water and the bilayer in a 5:5 EtOH:water mixture, using constrained MD [16, 17]. The free energy profiles are shown in Figure 4. In the bilayer in pure water, as the water molecule moves out of the bulk phase and approaches the bilayer there is an increase in the free energy, followed by a small local minimum that corresponds to the peak in the CER2 density profile. This local minimum is probably associated with the formation of H-bonds between the water molecule and the CER2 headgroups. As the water molecule moves into the hydrocarbon phase there is a further increase in the free energy until it reaches a maximum, which corresponds to the most densely packed, ordered region of the CER2 chains (see ESI Figure 6). The free energy then decreases towards a local minimum in the centre of the bilayer where the packing of the CER2 chains is less dense and the water molecule can be easily accommodated. Due to the symmetry of the bilayer in pure water, a water molecule that reaches the centre of the bilayer would most likely become trapped in this region due to the
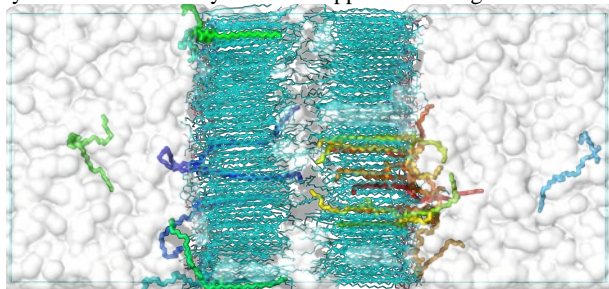

Figure 3 Snapshot of the bilayer in a 7:3 EtOH:water mixture. EtOH and water molecules are shown as white surfaces, CER2 molecules are shown as sticks with C atoms in cyan, O atoms in red, N atoms in blue and H atoms in white. CER2 molecules that have been either partially (one tail) or fully (both tails) extracted into the solvent layer are shown as different coloured thicker sticks.
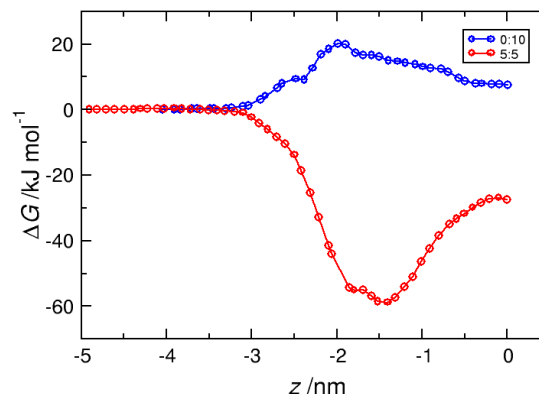

Figure 4 Free energy profile of a water molecule as a function of the perpendicular distance z between the water molecule and the centre of mass of the bilayer for the bilayers in pure water and a 5:5 EtOH:water mixture.

barrier to exit either leaflet. The overall shape of the free energy profile is similar to that observed for membranes of different lipid compositions [17, 18]; however the molecular structure of CER2 (absence of a bulky headgroup and asymmetrical chains) gives rise to the specific features of the "shoulder" in the headgroup region and a lower free energy minimum in the centre of the bilayer.

In the bilayer in a 5:5 EtOH:water mixture there is no longer a free energy barrier in the CER2 headgroup region. Instead it is strongly favourable for a water molecule to penetrate the bilayer and enter the most ordered region of the hydrocarbon chains. There is then an apparent relatively large barrier for the single water molecule to exit the dense hydrocarbon region and enter the interior of the membrane. As we observe spontaneous water permeation in the unconstrained MD simulation of a CER2 bilayer in a 5:5 EtOH:water mixture, it is not surprising that the free energy profile indicates a favourable thermodynamic pathway for water entry into the bilayer. The large free energy barrier to move the water molecule from the dense hydrocarbon phase into the membrane interior, however, suggests a disparity between our two approaches. Examination of the simulation trajectories shows that, in all of the constrained simulations, the water molecule diffuses in the plane of the bilayer until it reaches an EtOH-rich defect or pore, where it remains for the rest of the simulation. This confirms that the most favourable pathway for water is along an EtOH-induced defect or pore, rather than directly through the hydrocarbon phase. In the simulations corresponding to the region z = -2 nm to z = -1 nm, the water molecule resides in the large EtOH-induced pore. Whereas in the simulations corresponding to the region z = -1 nm to z = 0, the water molecule resides in smaller EtOH-induced defects. In other words, our free energy profile is not representative of a single pathway through the bilayer. One might expect that permeation through a large pore is overall more favourable than permeation along a small defect. Therefore, in the presence of defects or pores, a simple one-dimensional reaction coordinate may not provide the full picture of the permeation process as the timescales to diffuse (in the lateral direction) from a small defect to a large pore are inaccessible. Future work should therefore consider permeation in both the lateral and perpendicular directions. Indeed as we move to consider permeation of solutes such as drug molecules, other degrees of freedom such as the conformational freedom of the permeant, and factors such the de-polarization of the permeant should also be considered [19]. However identifying the most suitable simulation methodology to adequately capture these more complex permeation pathways remains a challenge.

The molecular structure of EtOH appears key to its mechanism of action. EtOH is amphiphilic with a hydrophilic hydroxyl group that can act as an H-bond donor or acceptor and a hydrophobic methyl group. When the CER2 bilayer is solvated in an EtOH:water mixture, EtOH accumulates at the bilayer interface where it displaces CER2-water H-bonds. Once at the interface an EtOH molecule may reorient such that the methyl group makes contact with the hydrocarbon region of the bilayer. Occasionally, another interfacial EtOH molecule H-bonds to the first EtOH molecule and then to the same CER2 headgroup, pushing the first EtOH deeper into the bilayer. Additional EtOH molecules can then join the chain in a similar way, which grows until the first EtOH molecule reaches the interior of the membrane and diffuses into the less-dense space. Water molecules are then able to traverse the defect; the EtOH molecules H-bond to the water molecule, while the methyl group shields the water molecule from the hydrocarbon chains. We propose that the crucial molecular features of EtOH that give rise to its mechanism of action are (i) its ability to act as an H-bond donor *and* acceptor, which facilitates accumulation at the interface and enables EtOH to form chains through the membrane by H-bonding with itself, and (ii) its amphiphilic character, which facilitates the first step of partitioning of EtOH into the hydrocarbon phase. EtOH is distinct from other amphiphilic PEs such as DMSO that cannot act as H-bond donors and cannot therefore form permeating networks with themselves through the membrane [12]. It will be interesting to extend this study to other amphiphilic PEs that can act as H-bond donors and acceptors, such as propylene glycol, which has been shown to cause the formation of pores in phospholipid bilayers [20].

Our study provides the first direct evidence for EtOH-induced pore formation in skin lipids. The idea that EtOH-enhanced membrane transport might occur *via* a porous pathway is not, however, entirely new. In the 1980's and 90's, inspired by the idea that extraction of lipids by EtOH could lead to an increase in porosity of the skin, data on drug penetration in the presence of EtOH was shown to fit best to theoretical models that allow for drug flux through multiple routes (*i.e.* both the lipid phase and transmembrane pores), compared to models that only allow for direct penetration through the lipid phase [2, 21]. The work presented here now provides a firm molecular-basis for these assumptions and could be used in the future to refine and infer parameters (such as pore radius and density) for theoretical membrane diffusion models.

Conclusions

We show for the first time that EtOH can induce the formation of defects and pores in CER2 bilayers, which may explain how EtOH enhances the permeability of molecules through skin and other biomembranes. Our proposed mechanism is entirely consistent with previous experimental observations that EtOH does not fluidise skin lipids at physiological temperatures and that it extracts lipids from the bilayer. Our results indicate that lipid extraction may play a role in the formation of nanometre-sized pores at high EtOH concentrations. Finally, we propose a set of molecular features necessary for the rational design of membrane modulators that enhance membrane permeation *via* defects or pores, while maintaining the overall structure and bulk phase behaviour of the unperturbed membrane.

Acknowledgements

Notes and references

*a*Department of Chemistry and Centre for Scientific Computing, University of Warwick, Gibbet Hill Road, Coventry, CV4 7AL. Email: r.notman@warwick.ac.uk

Electronic Supplementary Information (ESI) available: simulation methodology and analysis of the structural properties of the bilayers.

1. E. Terama, O. H. S. Ollila, E. Salonen, A. C. Rowat, C. Trandum, P. Westh, M. Patra, M. Karttunen and I. Vattulainen, *J. Phys. Chem. B*, 2008, **112**, 4131-4139; E. van den Brink-van der Laan, V. Chupin, J. A. Killian and B. de Kruijff, *Biochemistry*, 2004, **43**, 5937-5942.
2. E. Manabe, K. Sugibayashi and Y. Morimoto, *Int. J. Pharm.*, 1996, **129**, 211-221.
3. Á. Farkas and L. Kemény, *Br. J. Dermatol.*, 2010, **162**, 711-716.
4. T. Kai, V. H. W. Mak, R. O. Potts and R. H. Guy, *J. Control. Release*, 1990, **12**, 103-112.
5. A. C. Williams and B. W. Barry, *Adv. Drug Deliv. Rev.*, 2004, **56**, 603-618.
6. D. Bommannan, R. O. Potts and R. H. Guy, *J. Control. Release*, 1991, **16**, 299-304.
7. E. C. Guillard, A. Tfayli, C. Laugel and A. Baillet-Guffroy, *Eur. J. Pharm. Sci.*, 2009, **36**, 192-199.
8. S. Kwak, E. Brief, D. Langlais, N. Kitson, M. Lafleur and J. Thewalt, *BBA-Biomembranes*, 2012, **1818**, 1410-1419.
9. S. L. Krill, K. Knutson and W. I. Higuchi, *BBA-Biomembranes*, 1992, **1112**, 273-280.
10. M. Kranenburg and B. Smit, *FEBS Letters*, 2004, **568**, 15-18; J. Chanda and S. Bandyopadhyay, *Chem. Phys. Lett.*, 2004, **392**, 249-254; M. Patra, E. Salonen, E. Terama, I. Vattulainen, R. Faller, B. W. Lee, J. Holopainen and M. Karttunen, *Biophys. J.*, 2006, **90**, 1121-1135; A. N. Dickey and R. Faller, *Biophys. J.*, 2007, **92**, 2366-2376; A. A. Gurtovenko and J. Anwar, *J. Phys. Chem. B*, 2009, **113**, 1983-1992; A. Polley and S. Vemparala, *Chem. Phys. Lipids*, 2013, **166**, 1-11.
11. S. A. Pandit and H. L. Scott, *J. Chem. Phys.*, 2006, **124**, 014708; S. Guo, T. C. Moore, C. R. Iacovella, L. A. Strickland and C. McCabe, *J. Chem. Theory Comput.*, 2013, **9**, 5116-5126; C. Das, M. G. Noro and P. D. Olmsted, *Biophys. J.*, 2009, **97**, 1941-1951.
12. R. Notman, W. K. den Otter, M. G. Noro, W. J. Briels and J. Anwar, *Biophys. J.*, 2007, **93**, 2056-2068.
13. R. Notman, J. Anwar, W. J. Briels, M. G. Noro and W. K. den Otter, *Biophys. J.*, 2008, **95**, 4763-4771; R. Notman and J. Anwar, *Adv. Drug Deliv. Rev.*, 2013, **65**, 237-250.
14. W. L. DeLano, The PyMOL Molecular Graphics System, DeLano Scientific, San Carlos, CA, USA, 2002.
15. A. Tfayli, E. Guillard, M. Manfait and A. Baillet-Guffroy, *Analyst*, 2012, **137**, 5002-5010.
16. S. J. Marrink and H. J. C. Berendsen, *J. Phys. Chem.*, 1994, **98**, 4155-4168; M. Orsi and J. W. Essex, *Soft Matter*, 2010, **6**, 3797-3808.
17. D. Bemporad, J. W. Essex and C. Luttmann, *J. Phys. Chem. B*, 2004, **108**, 4875-4884.
18. J. P. M. Jämbeck and A. P. Lyubartsev, *J. Chem. Theory Comput.*, 2012, **9**, 774-784; C. L. Wennberg, D. van der Spoel and J. S. Hub, *J. Am. Chem. Soc.*, 2012, **134**, 5351-5361.
19. J. P. M. Jämbeck and A. P. Lyubartsev, *The Journal of Physical Chemistry Letters*, 2013, **4**, 1781-1787; J. P. M. Jambeck and A. P. Lyubartsev, *Phys. Chem. Chem. Phys.*, 2013, **15**, 4677-4686; I. Vorobyov, W. F. D. Bennett, D. P. Tieleman, T. W. Allen and S. Noskov, *J. Chem. Theory Comput.*, 2012, **8**, 618-628.
20. Z. E. Hughes, C. J. Malajczuk and R. L. Mancera, *J. Phys. Chem. B*, 2013, **117**, 3362-3375.
21. T. Inamori, A. H. Ghanem, W. I. Higuchi and V. Srinivasan, *Int. J. Pharm.*, 1994, **105**, 113-123; K. D. Peck, A. H. Ghanem and W. I. Higuchi, *Pharm. Res.*, 1994, **11**, 1306-1314; A.-H. Ghanem, H. Mahmoud, W. l. Higuchi, U. D. Rohr, S. Borsadia, P. Liu, J. L. Fox and W. R. Good, *J. Control. Release*, 1987, **6**, 75-83.